BANDWIDTH ENHANCEMENT OF MICROSTRIP PATCH ANTENNA USING JERUSALEM CROSS-SHAPED FREQUENCY SELECTIVE SURFACES BY INVASIVE WEED OPTIMIZATION APPROACH

F. Mohamadi Monavar[*] and N. Komjani

Department of Electrical Engineering, Iran University of Science and Technology, Tehran, Iran

Abstract—In this paper, we present a novel approach for improving the bandwidth of a microstrip patch antenna using Jerusalem cross-shaped frequency selective surfaces (JC-FSSs) as an artificial magnetic ground plane. The invasive weed optimization (IWO) algorithm is employed to derive optimal dimensions of the patch antenna and JC-FSS element in order for the whole structure to work at 5.8 GHz with consideration of gain. For the most efficient design, the antenna and FSS ground plane are optimized together, rather than as separate components. Simulation results demonstrate that this optimum configuration (the microstrip patch antenna over the artificial magnetic ground plane) have a broad bandwidth of about 10.44%. This wide bandwidth is obtained while the thickness of the whole structure is limited to 0.1λ. Further more desirable radiation characteristics have been successfully realized for this structure. The radiation efficiency of the AMC antenna configuration was found to be greater than 85% over the entire bandwidth. In general by introducing this novel Jerusalem cross artificial magnetic conductor (JC-AMC) in lieu of the conventional perfect electric conductor (PEC) ground plane, the bandwidth enhancement of about 67% and a thinner and lighter weight design has been obtained. Sample antenna and EBG layer are also fabricated and tested, to verify the designs. It is shown that the simulation data in general agree with the measurement results for the patch antennas implemented with FSS ground plane.

1. INTRODUCTION

Recently, with the growing number of wireless applications, there has been an increasing worldwide interest in low profile, low-cost, wideband system designs. One of the most intrinsic components of wireless systems is their antenna. Microstrip patch antennas due to their compactness and ease of fabrication are of particular interest for these systems. However one drawback of this antenna is its narrow bandwidth. This is due to the fact that the radiated field from the image of the antenna's electric current tends to cancel out the radiated field from the antenna current, which makes it difficult to match the antenna input impedance. It has been suggested that the bandwidth can be recovered by removing the conventional PEC ground plane and using a perfect magnetic conductor (PMC) instead. In this case the image of electric current is in-phase and parallel to the original current distribution. So the antenna impedance matching would be possible over a relatively wide bandwidth. Artificial magnetic conductor occasionally known as electromagnetic band gap (EBG) is a special member of high impedance surface (HIS) family, which is designed to imitate the behavior of a PMC. So far, several methods have been proposed to realize AMCs. One approach suggested is employing a 2D periodic metallic array at the interface of a metal-backed dielectric slab with or without vias connected to a PEC ground plane [1–9]. In previous research some narrowband antennas such as microstrip patches and dipoles have been mounted on EBG structures to improve their performance [10–16].

In this work we propose to design a patch antenna over a class of high impedance surface (HIS) substrates, using JC-shaped FSS. The objective in such design is to enhance the bandwidth of the microstrip antenna operating at the center frequency of 5.8 GHz. However, the design of such a complex structure is not an easy matter due to the many design parameters that require optimizing.

Invasive Weed Optimization (IWO) is one of the novel numerical stochastic optimization algorithms that is very apropos to this purpose. As shown in the recent literature (see for instance [17–20]), IWO has been successfully applied to determine a global minimum (or a maximum) of a multi-variables function representing the problem to be solved.

In this article, first different methods of designing a low profile antenna over AMC ground planes are presented in greater detail. After this we employ the IWO algorithm to determine the dimensions of the metallic elements of the FSS screen, feed position, and the geometry of the patch antenna. In order to analyze the scattering

properties of the structure, HFSS software is used. To verify the results experimentally, this structure is fabricated and tested. In Section 5 a parametric study is conducted in which the influence of changing the geometrical parameters of the FSS element on the antenna performance has been outlined and quantified. Finally a qualitative explanation of FSS behavior with the help of a simple circuit model is presented amc discussed.

2. METHODS OF DESIGNING ANTENNA-EBG SYSTEMS

When designing a low profile antenna over AMC ground Plane, several methods of optimization are possible. One approach suggested is to design antenna and EBG separately like those in [21–24]. In this case the PEC-backed, FSS-element configuration embedded in dielectric layers is considered. Then the thickness and the dielectric permittivity of each layer, together with the dimensions of the FSS element, are optimized in order to get the desired frequency response. Some other studies allow the shape of the FSS element to be included as an additional variable for optimization process. In this case the basic periodicity cell is subdivided into elementary pixels coded as 1s representing the presence of metal or 0s representing the absence of metal. Then a binary-coded GA is used to optimize these parameters to achieve a PMC-like performance, characterized by a reflection coefficient magnitude of 1 and phase of 0 [25–27].

According to [28, 29], and [30], this method besides its rewards, is very time-consuming and not always leading to the best design. Another disadvantage of such design is, when putting antenna over this AMC ground plane, either a frequency shift occurs or a loss in gain is observed. It is due to the fact that the resulting performance is not just a linear combination of the individual antenna and ground plane performances. So in order for the combination to achieve the best performance, many parameters must be readjusted [31]. Another approach is to optimize antenna-AMC ground plane simultaneously. In this case the optimization time can be noticeably reduced. As shown in [31], this procedure will result in a useful antenna-EBG system design with better overall performance. It must be noted that even in this case, considering a pixilated FSS screen will increase the time and the complexity of the problem, besides not always leading to the best design.

A proof to this could be found in [28], where a skewed cross (SC) based AMC is extracted from previously GA-designed AMC by utilizing simple parametric studies together with simple and fast

optimization. It is worth noting that, this new structure yields very good angular stability, smaller cell size and satisfactory BW. A more in-depth development of the JC-FSS from a GA-designed AMC is presented in [29], where a novel 3D AMC utilizing a 2-layer JC-FSS is obtained that yields smaller cell size and thickness with better angular stability in comparison with the GA-designed one. According to what mentioned above, we use the second approach based on choosing a fixed screen geometry rather than a pixelized grid. The well known JC-FSS is used. JC-FSSs, have been successfully employed in a whole host of applications, such as filters, polarizes, phase shifters, etc. Recently they have been extensively investigated by researchers to act as HIS. It is due to the fact that, JC-based AMCs are able to be designed to show more angular stability relative to the rivals when illuminated obliquely [32, 33].

3. IWO OPTIMIZATION OF ANTENNA-AMC GROUND PLANE

3.1. Antenna over PEC

In the present section we consider performance of a patch antenna over the JC-shaped AMC ground plane. Then compare its performance with a traditional patch over a PEC surface. For the sake of a fair comparison, we use the same size patch and ground plane in both cases. The geometry of the conventional patch, etched on 1.58 mm
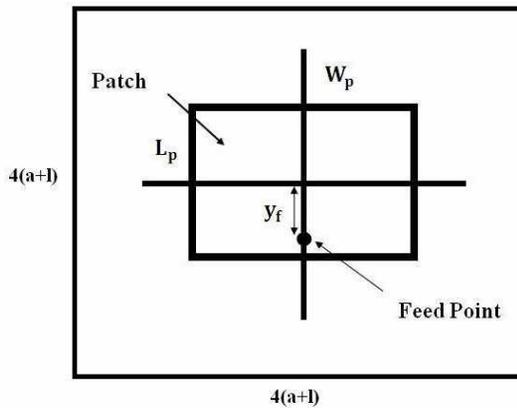

Figure 1. The reference patch antenna on the conventional substrate. Ground plane is $4(a + l) \times 4(a + l)$ mm.

thick Rogers RT/duroid6002 substrate and mounted over the PEC ground plane is shown in Figure 1. The antenna is fed by a $50\,\Omega$ coaxial probe through a SMA connector. To assess the bandwidth-improvement characteristics, this antenna will be modified, using AMC ground plane in lieu of the conventional PEC ground plane.

3.2. Antenna over AMC

We start with the basic periodicity cell of the JC-shaped AMC shown in Figure 2. The dielectric material used for the AMC substrate is RT Duroid6002 ($\varepsilon_r = 2.94$) and the thickness chosen to be 3.16 mm. All the parameters (a, l, w, W) depicted in Figure 2 except g, are used as optimization variables. Where W and $(a-g)/2$ are length and width of the edge parts while l and w indicate the length and width
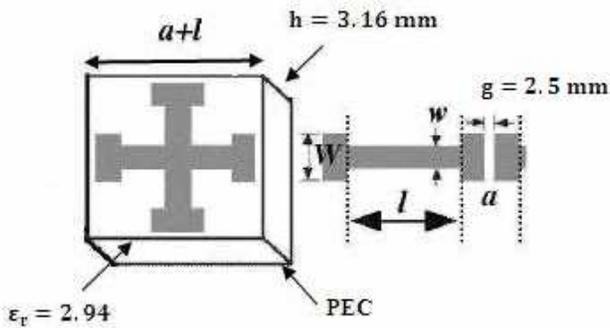

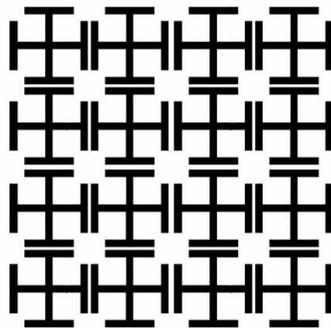**Figure 2.** The unit cell geometry for the JC-shaped AMC.

Figure 3. Periodic HIS substrate which is a 4×4 finite array of JC-FSS unit cells printed on the PEC-backed dielectric material.
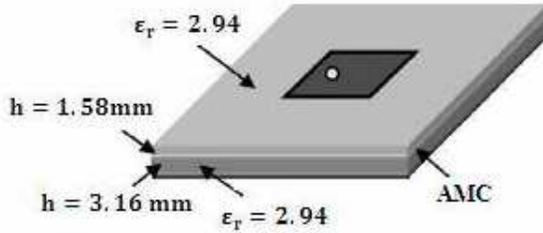
Figure 4. The geometry of patch antenna located over the EBG ground plane for a broadband antenna-EBG system. EBG cells are $(a + l) \times (a + l)$ mm with a spacing of 2.5 mm, $4(a + l) \times 4(a + l)$ mm ground plane.

of the straight portion of cross respectively. A complete view of the FSS screen which is a 4×4 grid of the JC-FSS unit cells as shown in Figure 3 is used as AMC ground plane. Therefore the overall size of the ground plane would be $4(a + l) \times 4(a + l)$. To allow for feeding the antenna a gap in between two unit cells is considered $g = 2.5$ mm.

Figure 4 shows the geometry of a patch antenna printed exactly above the center of this finite EBG ground plane. Now we employ the IWO algorithm in an attempt to optimize the antenna-EBG system under the following circumstances.

3.2.1. Optimization Objective

Best impedance matching at resonant frequency of 5.8 GHz.

3.2.2. Optimization Variables

The length L_p, width W_p and the location of the feed probe y_f of the patch antenna as well as dimensions of JC-FSS w, W, a, l (see Figures 1 and 2).

As such, the dimension of the solution space is seven. Each of these parameters constrained to the specific range from P_{min} to P_{max}, where P_{min} and P_{max} are the minimum and maximum range bounds corresponding to the parameter P. During optimization process, these parameters modified and changed within their particular range in which to search for the optimal solution.

Having chosen a particular range for each variable, the IWO optimization begins by creating an initial population and then calculating fitness values. The fitness value returned by the fitness function is proportional to the *goodness* of a given trial solution.

In addition, it is necessary to include the following constraints:

$W/l < 0.8$ To maintain the JC shaped AMC.

$W_p < 4(a + l)$ Patch cannot cross the ground plane.

$y_f < L_p/2$ Feed cannot go beyond the patch.

An initial population size of 10 is used and the number of generations is set to 100.

It is clear that faster convergence might occur when starting from a good initial population. In this problem, we create the initial population by using the best individuals of several trial populations. In this way acceptable design is obtained before 100 generations. The parameters of the optimized structure are listed in Table 1.

The simulated return loss of this structure is plotted in Figure 5. As can be seen from this figure the antenna resonance is found to be at 5.8 GHz and it exhibits a very wide bandwidth of about 10.44%. To illustrate the enhancement in bandwidth, the return loss of the conventional patch antenna over the same size PEC ground plane was also obtained. It demonstrated a narrow bandwidth of about $BW = 3.91\%$ around 6.26 GHz. For the sake of fair comparison, following the approach used in [21] we allow the permittivity of the substrate of the conventional patch to be a variable to achieve the same resonant frequency.

To this end, the conventional patch was designed on a Taconic RF-35 substrate with $\varepsilon_r = 3.5$. The return loss of this antenna together with the one for antenna over AMC is shown in Figure 5. As can be seen from this figure, the conventional patch antenna in this case shows a narrow bandwidth of 3.44% around 5.8 GHz. We observe that when an IWO/FSS ground plane is employed, with the same resonant frequency, we have $\approx 67\%$ increase in bandwidth. The simulated gain and efficiency of the patch antenna on the HIS together with

Table 1. Geometrical parameters of the antenna-AMC structure.

Parameter	Optimized Value (mm)
L_p	12.5
y_f	5
W_p	17.5
w	0.55
W	8.5
a	4.31
l	11.64

the antenna on PEC are plotted in Figures 6 and 7, respectively. As seen in these plots, for the patch antenna over the IWO optimized AMC ground plane, the gain is above 5 dB over the range of 5.527 to 6.015 GHz, or a 8.41% bandwidth with a peak of 6.57 dB where as the efficiency is greater than 85% over the entire bandwidth of 5.5 to 6.13 GHz.

The radiation patterns of both patch antennas at 5.8 GHz are plotted in Figure 8.

To verify the conclusions drawn from the simulation, the design of the patch antenna on the AMC is fabricated and tested. Figure 9 shows a photograph of the EBG structure together with the fabricated antenna. The measured return loss of the antenna on the EBG together with the simulation results are plotted in Figure 10. It is observed that
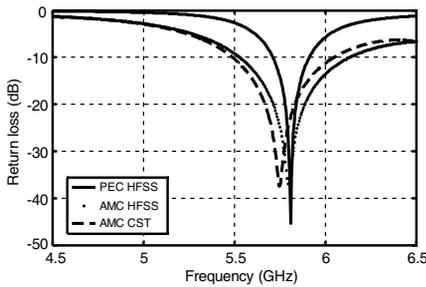
Figure 5. Comparison of S_{11} characteristics of the patch antenna: Over the PEC ground plane and on the IWO optimized AMC substrate.
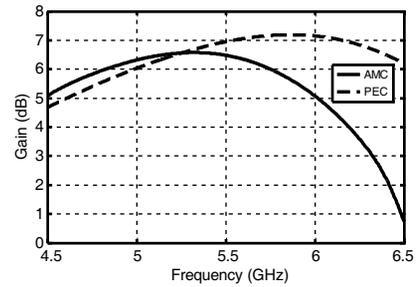

Figure 6. Comparison of simulated gain versus frequency for the patch antenna: Over the PEC ground plane and on the IWO optimized AMC ground plane.
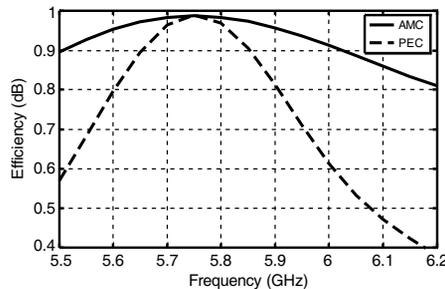

Figure 7. Comparison of simulated efficiency versus frequency for the patch antenna: Over the PEC ground plane and on the IWO optimized AMC ground plane.
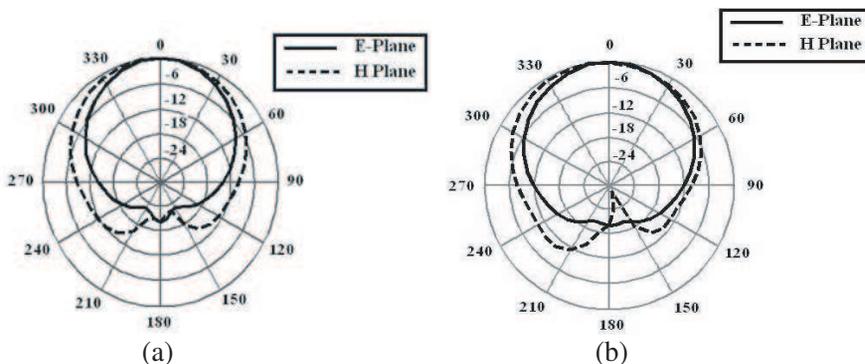
Figure 8. Radiation patterns of patch antenna at operating frequency of 5.8 GHz over the (a) conventional and (b) HIS substrates.
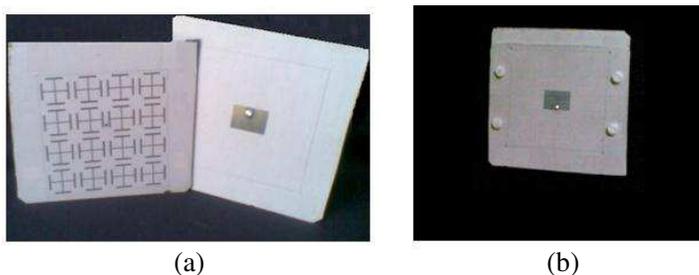

Figure 9. Photo of microstrip patch antenna on the EBG structure. (a) Intermediary stage. (b) Completed antenna structure.

the antenna resonates at 5.9 GHz and its -10 dB impedance bandwidth is from 5.626 to 6.24 GHz or 10.41%. The measured radiation patterns for this dual-layer antenna with the EBG ground plane are shown in Figure 11. As seen in these plots, the agreement between the measured and simulated results is excellent. From this experimental demonstration, it can be concluded that a significant improvement in antenna performance can be achieved by utilizing an EBG surface.

4. PARAMETRIC STUDY

Among the parameters which affect the gain and return loss characteristics of the AMC-antenna structure, the geometry of the FSS elements is the most important one. In the following, we study the effect of geometrical parameters of the FSS element (W, l, w, a). By changing these parameters within the range of 10%–20% of their
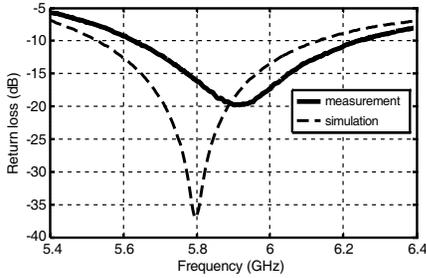
Figure 10. Simulated and measured S_{11} versus frequency for patch antenna over the HIS substrate.
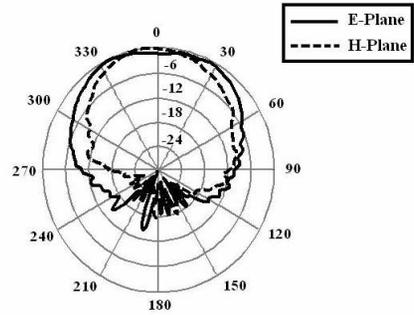
Figure 11. Measured radiation patterns of patch antenna over the EBG AMC ground plane at the center frequency of 5.8 GHz for two main cuts ($\varphi = 0°$ and $\varphi = 90°$).

Table 2. Resonant frequency and bandwidth for the antenna-AMC structure for varying the FSS parameter W.

W (mm)	f_r (GHz)	BW
7.5	6	10% (5.73–6.33 GHz)
8.5	5.8	10.44% (5.525–6.13 GHz)
9.5	5.55	10.09% (5.31–5.87 GHz)

Table 3. Resonant frequency and bandwidth for the antenna-AMC structure for varying the FSS parameter a.

a (mm)	f_r (GHz)	BW
3.31	6.07	10.05% (5.8–6.41 GHz)
4.31	5.8	10.44% (5.525–6.13 GHz)
5.31	5.59	10.02% (5.34–5.9 GHz)

optimum values, we examine their effects on the gain and return loss of the antenna. At each step, only one parameter is changed while the others have been kept constant. Tables 2–5 list the resonant frequency together with the BW confirmed with numerical analysis in HFSS.

Table 4. Resonant frequency and bandwidth for the antenna-AMC structure for varying the FSS parameter l.

l (mm)	f_r (GHz)	BW
9.64	5.88	10.03% (5.63–6.22 GHz)
11.64	5.8	10.44% (5.525–6.13 GHz)
13.64	5.62	9.96% (5.37–5.93 GHz)

Table 5. Resonant frequency and bandwidth for the antenna-AMC structure for varying the FSS parameter w.

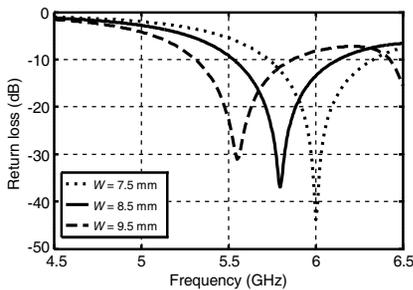| w (mm)	f_r (GHz)	BW
0.45	5.76	10.59% (5.49–6.1 GHz)
0.55	5.8	10.44% (5.525–6.13 GHz)
0.65	5.83	9.95% (5.57–6.15 GHz)

Figure 12. Return loss of patch antenna over the HIS substrate for different strip width W.
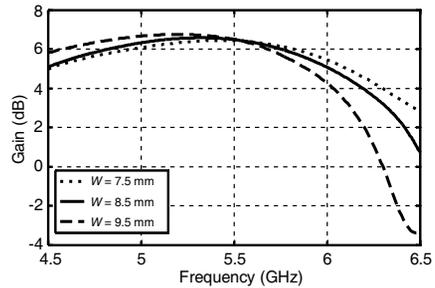

Figure 13. Simulated gain versus frequency for patch antenna over the HIS substrate for different strip width W.

4.1. Effect of Changing of the W

The results concerning the return loss and gain of the antenna for a strip width variation are shown in Figures 12 and 13 respectively. The results reveal that increasing the strip width shifts down the resonant frequency and vice versa.

4.2. Effect of Changing of the a

A similar effect, compared to a variation of the strip width can be observed when the parameter a is increased. Here increasing a leads
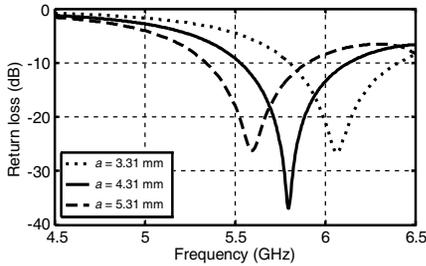
Figure 14. Return loss of patch antenna over the HIS substrate for different values of a.
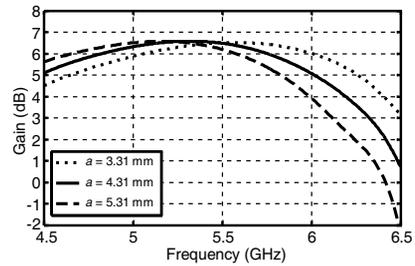

Figure 15. Simulated gain versus frequency for patch antenna over the HIS substrate for different values of a.
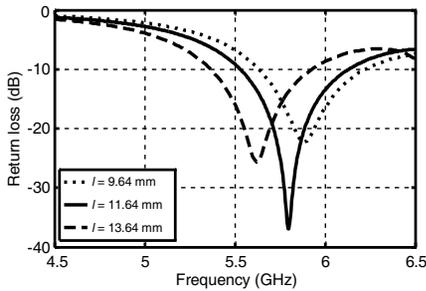

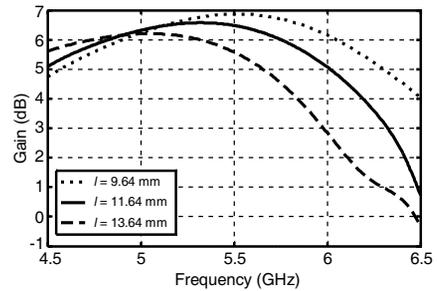**Figure 16.** Return loss of patch antenna over the HIS substrate for different length l.

Figure 17. Simulated gain versus frequency for patch antenna over the HIS substrate for different length l.

to a decreasing resonant frequency of the antenna. The corresponding results for a variation of a are shown in Figures 14 and 15.

4.3. Effect of Changing of the Length l

As it is apparent from Figure 16 and Table 4, an increase of length l implies a reduction of the fractional bandwidth together with the good matching characteristics shift to lower frequencies. The result concerning the gain is also depicted in Figure 17.

4.4. Effect of Changing of the w

In contrast to the previous results, an increase of w corresponds to an increase in resonance frequency as one could infer by observing Figure 18 and Table 5. Gain variation is negligible as can be seen in Figure 19.
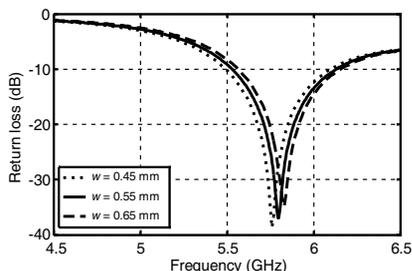
Figure 18. Return loss of patch antenna over the HIS substrate for different values of w.
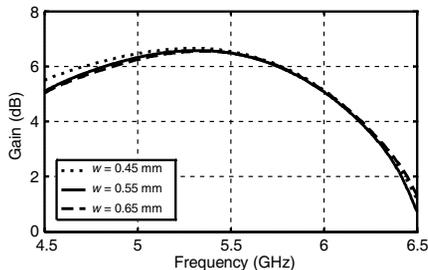

Figure 19. Simulated gain versus frequency for patch antenna over the HIS substrate for different values of w.

In the previous section, the influence of changing the geometrical parameters of the FSS element on the antenna performance was outlined and quantified. We observed that by increasing W, a, and l as well as decreasing w the good matching characteristics shift to lower frequencies. Actually the resonant frequency of the whole structure is a function of ε_{reff}. Here incorporating FSS cells into the substrate will result in the new ground plane. The relative permittivity of this new substrate is a function of FSS cell geometry. So the change in resonant frequency of antenna is due to the change in ε_{reff} which results from changing the FSS dimensions. Changing the FSS parameters will also affect the antenna bandwidth. It happens because changing the parameters in this manner will reduce the BW and resonant frequency of the reflection phase of the EBG. This fact can be qualitatively explained by considering formulas obtained from the static (TEM/quasi-TEM) wave theory as follows.

5. ANALYTICAL MODEL

To get more insight in the results that have been derived up to now, the further analysis will concentrate on a theoretical study on frequency selective surfaces (FSSs) using simple circuit models presented in previous literature to predict BW and resonant frequency for some specific AMCs. For the grid of metal Jerusalem crosses, one can find equivalent circuit models in [32–35]. First of all we want to take a look at the circuit model and the formulas for resonant frequency and BW presented in [34]. Note that the circuit model is depicted along one axis. It is due to the fact that Jerusalem cross is a symmetric shape
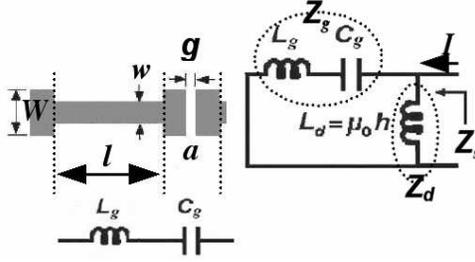
Figure 20. The approximate circuit model for the proposed JC-FSS unit cell.

and the performance is the same along both axes.

$$f_r = \frac{1}{2\pi\sqrt{(L_g + L_d)C_g}} \tag{1}$$

$$BW = \frac{\pi}{8\eta_0}\sqrt{\frac{L_g + L_d}{C_g}} \times \left(\frac{L_d}{L_g + L_d}\right)^2 \tag{2}$$

Formulas for L_g, C_g, and L_d can be found in [34] and will be not repeated further for the sake of brevity. Referring to the configuration depicted in Figure 20, it is apparent that the grid effective inductance L_g (due to straight portions of crosses) is, evidently, related to l and w whereas the effective capacitance C_g (due to the strong capacitive coupling of adjacent crosses) is proportional to W and a. At this point we can draw the conclusion that increasing W and a, results in an increase of the capacitance C_g which based on relation (1) and (2) leads to reducing the resonant frequency and BW of the FSS structure. A closer look to (1) and (2) reveals that an increase of the length l as well as decreasing w, implies a small degradation of the bandwidth of the structure while decreases the resonant frequency due to the enlargement of the inductance L_g.

6. CONCLUSION

In this paper a novel design of artificial magnetic conductor substrate for bandwidth enhancement of patch antenna is proposed. Making use of the HIS, mutual coupling between the antenna and its image is reduced dramatically which results in ease of impedance matching over a relatively wide bandwidth as well as total power reflection that creates the desired front-to-back ratio. The AMC-Antenna design has been derived using the IWO with a view to improve the bandwidth

performance and radiation characteristics at the resonant frequency. Desirable bandwidth and radiation patterns have been successfully realized for this structure. A parametric study was also conducted to evaluate the Antenna-AMC performance while changing the FSS geometrical parameters. It was shown that the circuit model for JC-FSS can be of great help while analyzing the whole system behavior. Finally the patch antenna over an AMC substrate was fabricated and tested. It was demonstrated that a return loss bandwidth of about 10.44% and a gain bandwidth of 8.41% are possible. Therefore the overall bandwidth of the system is considered to be from 5.527 GHz to 6.015 GHz or 8.41% with a center frequency of 5.8 GHz. The radiation efficiency of the AMC antenna configuration was found to be greater than 85% over the whole impedance bandwidth.

ACKNOWLEDGMENT

REFERENCES

1. He, Y., L. Li, C.-H. Liang, and Q. H. Liu, "EBG structures with fractal topologies for ultra-wideband ground bounce noise suppression," *Journal of Electromagnetic Waves and Applications*, Vol. 24, No. 10, 1365–1374, 2010.

2. Zhang, J. C., Y. Z. Yin, and J. P. Ma, "Powell optimization of circular ring frequency selective surfaces," *Journal of Electromagnetic Waves and Applications*, Vol. 24, No. 4, 485–494, 2010.

3. Kawakatsu, M. N., V. A. Dmitriev, and S. L. Prosvirnin, "Microwave frequency selective surfaces with high Q-factor resonance and polarization insensitivity," *Journal of Electromagnetic Waves and Applications*, Vol. 24, Nos. 2–3, 261–270, 2010.

4. Kim, Y. J., K. B. Yang, and Y. S. Kim, "Wideband simultaneous switching noise suppression in mobile phones using miniaturized electromagnetic bandgap structures," *Journal of Electromagnetic Waves and Applications*, Vol. 24, Nos. 14–15, 1929–1938, 2009.

5. Lu, B., S.-X. Gong, J. Ling, and X. Wang, "The design and performance of a novel square-loop patch frequency selective surface," *Journal of Electromagnetic Waves and Applications*, Vol. 24, Nos. 8–9, 1085–1092, 2009.

6. Yeo, J. and D. Kim, "Novel tapered AMC structures for backscattered RCS reduction," *Journal of Electromagnetic Waves and Applications*, Vol. 23, Nos. 5–6, 697–709, 2009.

7. Lin, X. Q., T. J. Cui, Y. Fan, and X. Liu, "Frequency selective surface designed using electric resonant structures in terahertz frequency bands," *Journal of Electromagnetic Waves and Applications*, Vol. 23, No. 1, 21–29, 2009.

8. Sievenpiper, D., L. Zhang, R. F. J. Broas, N. G. Alexopolous, and E. Yablonovitch, "High-impedance electromagnetic surfaces with a forbidden frequency band," *IEEE Trans. Microw. Theory Tech.*, Vol. 47, No. 11, 1999.

9. Radisic, V., Y. Qian, R. Coccioli, and T. Itoh, "Novel 2-D photonic bandgap structure for microstrip lines," *IEEE Microw. Guid. Wave Lett.*, Vol. 8, No. 2, 1998.

10. Erdemli, Y. E., K. Sertel, R. A. Gilbert, D. E. Wright, and J. L. Volakis, "Frequency selective surfaces to enhance performance of broad band reconfigurable arrays," *IEEE Transactions on Antennas and Propagation*, Vol. 50, 1716–1724, Dec. 2002.

11. Luo, G. Q., W. Hong, H. J. Tang, J. X. Chen, X. X. Yin, Z. Q. Kuai, and K. Wu, "Filtenna consisting of horn antenna and substrate integrated waveguide cavity FSS," *IEEE Transactions on Antennas and Propagation*, Vol. 55, 92–98, Jan. 2007.

12. Chen, H. Y., Y. Tao, K. L. Hung, and H. T. Chou, "Bandwidth enhancement using dual-band frequency selective surface with Jerusalem cross elements for 2.4/5.8 GHz WLAN antennas," *IEEE International Conference on Wireless Information Technology and Systems (ICWITS)*, 2010.

13. Hiranandani, M. A., A. B. Yakovlev, and A. A. Kishk, "Artificial magnetic conductors realized by frequency-selective surfaces on a grounded dielectric slab for antenna applications," *IEE Pro. Microw. Antennas Propagat.*, Vol. 153, No. 5, 487–493, Oct. 2006.

14. Liang, J. and H. Y. D. Yang, "Radiation characteristics of a microstrip patch over an electromagnetic bandgap surface," *IEEE Transactions on Antennas and Propagation*, Vol. 55, No. 6, 1691–1697, Jun. 2007.

15. Ling, J., S.-X. Gong, B. Lu, H.-W. Yuan, W.-T. Wang, and S. Liu, "A microstrip printed dipole antenna with UC-EBG

ground for RCS reduction," *Journal of Electromagnetic Waves and Applications*, Vol. 23, Nos. 5–6, 607–616, 2009.

16. Gonzalo, R., P. D. Maagt, and M. Sorolla, "Enhanced patch-antenna performance by suppressing surface waves using photonic-bandgap substrates," *IEEE Trans. Microw. Theory Tech.*, Vol. 47, No. 11, 1999.

17. Mehrabian, A. R. and C. Lucas, "A novel numerical optimization algorithm inspired from weed colonization," *Ecological Informatics*, Vol. 1, 355–366, 2006.

18. Mallahzadeh, A. R., S. Es'haghi, and A. Alipour, "Design of an E-shaped MIMO antenna using IWO algorithm for wireless application at 5.8 GHz," *Progress In Electromagnetics Reseach*, Vol. 90, 187–203, 2009.

19. Mallahzadeh, A. R., H. Oraizi, and Z. Davoodi-Rad, "Application of the invasive weed optimization technique for antenna configurations," *Progress In Electromagnetics Research*, Vol. 79, 137–150, 2008.

20. Bahreini, B., A. R. Mallahzadeh, and M. Soleimani, "Design of a meander-shaped MIMO antenna using IWO algorithm for wireless applications," *Applied Computational Electromagnetics (ACES)*, Vol. 25, No. 7, 631–638, Jul. 2010.

21. Mosallaei, H. and K. Sarabandi, "Antenna miniaturization and bandwidth enhancement using a reactive impedance substrate," *IEEE Transactions on Antennas and Propagation*, Vol. 52, 2403–2414, Sep. 2004.

22. Yang, F. and Y. Rahmat-Samii, "Reflection phase characterizations of the EBG ground plane for low profile wire antenna applications," *IEEE Transactions on Antennas and Propagation*, Vol. 51, 2691–2703, Oct. 2003.

23. Qu, D., L. Shafai, and A. Foroozesh, "Improving microstrip patch antenna performance using EBG substrates," *IEE Proc. Microw. Antennas Propag.*, Vol. 153, No. 6, Dec. 2006.

24. Abedin, M. F., M. Z. Azad, and M. Ali, "Wideband smaller unit-cell planar EBG structures and their application," *IEEE Transactions on Antennas and Propagation*, Vol. 56, 903–908, Mar. 2008.

25. Mittra, Y. R. and S. Chakravarty, "A GA-based design of electromagnetic bandgap (EBG) structures utilizing frequency selective surfaces for bandwidth enhancement of microstrip antennas," *IEEE Antennas Propag. Soc. Int. Symp.*, 400–403, San Antonio, TX, 2002.

26. Monorchio, A., G. Manara, and L. Lanuzza, "Synthesis of artificial magnetic conductors by using multilayered frequency selective surfaces," *IEEE Antennas Wireless Propag. Lett.*, Vol. 1, 196–199, 2002.

27. Kern, D., D. H. Werner, A. Monorchio, L. Lanuzza, and M. Wilhelm, "The design synthesis of multiband artificial magnetic conductors using high impedance frequency selective surfaces," *IEEE Transactions on Antennas and Propagation*, Vol. 53, 8–17, Jan. 2005.

28. Hosseini, M., A. Pirhadi, and M. Hakkak, "Compact angularly stable AMCs utilizing skewed cross-shaped FSSs," *Microw. Opt. Tech. Lett.*, Vol. 49, No. 4, 781–786, Apr. 2007.

29. Hosseini, M., A. Pirhadi, and M. Hakkak, "A novel AMC with little sensitivity to the angle of incidence using 2-layer Jerusalem cross FSS," *Progress In Electromagetics Research*, Vol. 64, 43–51, 2006.

30. Hosseini, M., A. Pirhadi, and M. Hakkak, "Design of a novel AMC with little sensitivity to the angle of incidence and very compact size," *IEEE Antennas Propag. Soc. Int. Symp.*, 1939–1942, Albuquerque, NM, 2006.

31. Akhoondzadeh-Asl, L., D. J. Kern, P. S. Hall, and D. H. Werner, "Wideband dipoles on electromagnetic bandgap ground planes," *IEEE Transactions on Antennas and Propagation*, Vol. 55, 2426–2434, Sep. 2007.

32. Simovski, C. R., P. de Maagt, and I. V. Melchakova, "High-impedance surfaces having stable resonance with respect to polarization and incidence angle," *IEEE Transactions on Antennas and Propagation*, Vol. 53, 908–914, Mar. 2005.

33. Hosseini, M., A. Pirhadi, and M. Hakkak, "Design of an AMC with little sensitivity to angle of incidence using an optimized Jerusalem cross FSS," *Proc. IEEE Int. Workshop on Antenna Technology, Small Antennas, Novel Metamaterials*, 245–248, New York, 2006.

34. Hosseini, M. and M. Hakkak, "Characteristics estimation for Jerusalem cross-based artificial magnetic conductors," *IEEE Antennas Wireless Propag. Lett.*, Vol. 7, 58–61, 2008.

35. Andersson, I., "On the theory of self-resonant grids," *The Bell System Technical Journal*, Vol. 55, 1725–1731, 1975.